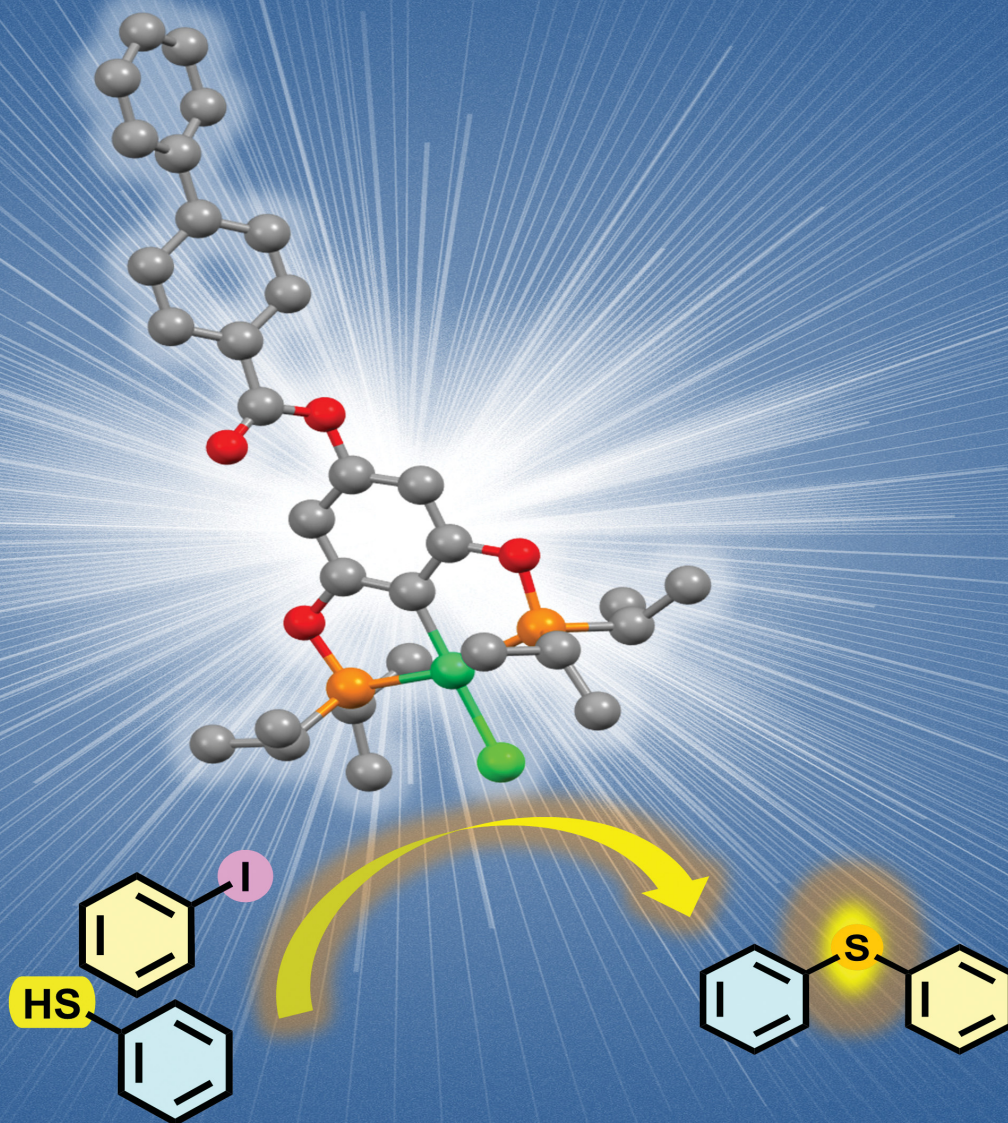


NJC

New Journal of Chemistry
rsc.li/njc

A journal for new directions in chemistry



ISSN 1144-0546

PAPER

David Morales-Morales *et al.*
Naphthyl and biphenyl *para*-substituted POCOP-Ni(II) pincer
complexes as efficient catalysts in C–S cross-coupling
reactions



Cite this: *New J. Chem.*, 2025, 49, 3426

Naphthyl and biphenyl *para*-substituted POCOP-Ni(II) pincer complexes as efficient catalysts in C–S cross-coupling reactions†

Luis E. López-Robledo,^a Evelin E. Ortiz-Fuentes,^a Ernesto Rufino-Felipe,^{‡a} Juan S. Serrano-García,^{‡a} Antonino Arenaza-Corona,^{‡a} Simón Hernandez-Ortega,^a Hugo Valdés,^b Lucero Gonzalez-Sebastian,^{‡c} Viviana Reyes-Márquez,^{‡d} and David Morales-Morales^{‡a*}

Received 27th August 2024,
Accepted 31st October 2024

DOI: 10.1039/d4nj03776f

rscl.li/njc

A series of six novel *para*-poly-aromatic acyl-functionalized nickel POCOP-pincer complexes, [NiCl(C₆H₂-4-Y-2,6-(OPR₂)₂)] (Y = [1,1'-biphenyl]-4-carboxylate, 2-naphthoate, R = ⁱPr, ^tBu, Ph), have been synthesized in a straightforward manner in high yields. All new complexes have been fully characterized by standard techniques and three of them unequivocally confirmed by single crystal X-ray diffraction analysis. The catalytic activity of the complexes was examined in C–S cross coupling reactions of iodobenzene with both aryl and alkyl thiols showing high conversions with low catalyst loadings.

Introduction

Pincer metal complexes provide robust architectures that continue to find notable applications in organometallic chemistry and homogenous catalysis.^{1–15} In particular, *mer*-tridentate ligands bearing aromatic backbones enable efficient fine-tuning of their electronic properties by substitution on the aryl moiety with either electron-donating or electron-withdrawing groups. Besides, the functionalization of the main framework with suitable groups allows the introduction of molecular recognition sites and the immobilization of these pincer complexes to solid supports. In this sense, some pincer complexes bearing anchoring groups (*i.e.* connectors) such as –OH, –NR₂, –OSiR₃ or halogens have been reported as precursors for preparing hybrid materials, such as metallodendrimers, and

heterogeneous catalysts *via* their immobilization on *e.g.*, silica or polymers.^{16–18} Hence, these hybrid materials have been successfully used as catalytic materials in both homogeneous and heterogeneous catalysis and materials science.^{19–31} In this context, Bergbreiter *et al.* prepared a *para*-NH₂ functionalized SCS-Pd pincer complex, which was subsequently attached to a soluble polymer support, polyethylene glycol, affording a highly stable and recyclable catalyst for the Heck reaction (Chart 1).³² Other interesting examples have been described by van Koten *et al.*, who synthesized a series of cationic *para*-substituted NCN-Pd pincer complexes using a strategically substituted group bearing two anchoring points, which allowed both the immobilization (–SMe₃) and introduction of an additional functional group (Y). These functionalized NCN-Pd complexes were successfully used as catalysts in the aldol reaction between methyl isocyanoacetate and various substituted benzaldehydes, achieving moderate conversions (Chart 1).³³ Noteworthy, the above-described species were prepared by the initial *para*-functionalization of the free ligands, followed by their metalation in multistep synthetic routes that produced pincer complexes, albeit in low yields.

Recently, we have become interested in the chemistry of *para*-substituted aryl phosphine-based pincers as an extension of our related work with POCOP-based variants. This interest has been motivated by the potential to exploit additional reaction control for the unique steric profile of these complexes through the functionalization of the main framework. In 2015, we reported the synthesis of a series of *para*-ester substituted Ni-POCOP pincer complexes (Chart 1).³⁴ We have extended this work to novel pincer platforms to explore their organometallic

^a Instituto de Química, Universidad Nacional Autónoma de México, Circuito Exterior, Ciudad de México, CP 04510, Mexico. E-mail: damor@unam.mx; Fax: +52-5556162217; Tel: +52-5556224514

^b Departamento de Química Orgánica y Química Inorgánica, Instituto de Investigación Química “Andrés M. del Río” (IQAR), Facultad de Farmacia, Universidad de Alcalá, Alcalá de Henares, 28805 Madrid, Spain

^c Universidad Autónoma Metropolitana-Iztapalapa, Av. San Rafael Atlixco No. 186, Ciudad de México, C.P. 09340, Mexico

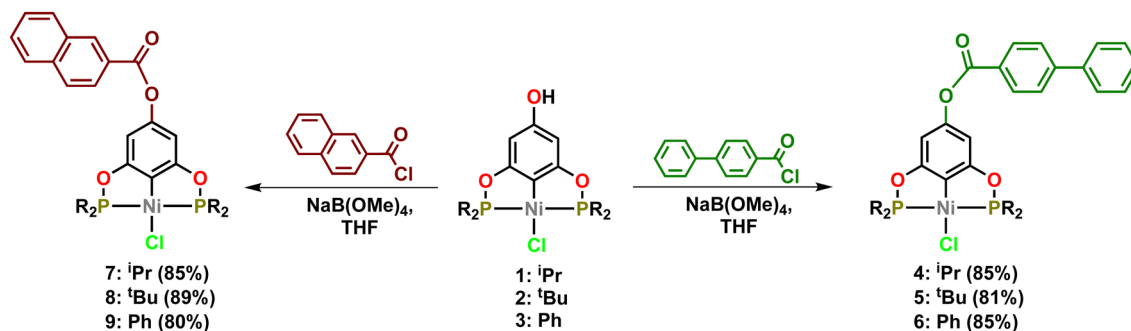
^d Departamento de Ciencias Químico-Biológicas, Universidad de Sonora, Luis Encinas y Rosales s/n, Hermosillo 83000, Sonora, Mexico

† Electronic supplementary information (ESI) available. CCDC 2062939–2062941. For ESI and crystallographic data in CIF or other electronic format see DOI: <https://doi.org/10.1039/d4nj03776f>

‡ Current address: Facultad de Farmacia, Universidad Autónoma del Estado de Morelos, Av. Universidad 1001, Chamilpa, Cuernavaca, Morelos, CP 62209, Mexico.



New J. Chem., 2025, **49**, 3426–3435 | 3427



Scheme 1 Synthesis of *para*-functionalized POCOP-Ni(II) pincer complexes.

further structural information exhibiting signals of the metalated C–Ni carbon as apparent triplets due to their coupling with the mutually *trans*-phosphorous nuclei at 123.2–121.4 ppm with values of $^2J_{\text{CP}}$ between 21–24 Hz. In addition, the presence of the C=O from the ester group was evidenced by its characteristic signal between δ 165.2–164.9 ppm. The FT-IR spectra of the series of complexes exhibited a key band between 1735 and 1722 cm^{-1} assigned to $\nu\text{C}=\text{O}$. Mass spectra also confirmed the formation of the complexes, the resulting spectra exhibiting the molecular ions $[\text{M}]^+$ at 741, 605, 661, 766, 631 and 688 m/z for complexes 4, 5, 6, 7, 8 and 9, respectively. The results obtained from elemental analysis of all the compounds are also in agreement with the proposed structural formulations.

X-Ray diffraction analysis

It was possible to obtain three crystalline structures of the complexes 4, 8 and 9. Crystals of complex 4 were obtained by

slow evaporation from a saturated dichloromethane solution, while those of complexes 8 and 9 were produced from their corresponding concentrated toluene solutions at room temperature. All compounds crystallized in a monoclinic system. The asymmetric unit of crystal 4 consists of two molecules of the pincer compound and two molecules of dichloromethane. Complex 8 crystallized with a molecule of toluene, while complex 9 crystallized without dissolvent. The crystallographic data of the compounds are summarized in Table S1 (ESI[†]) and the selected bond distances are listed in Table S2 (ESI[†]). The molecular structures of the compounds are shown in Fig. 1.

The carbon–nickel (C–Ni) bond distances were found to be around 1.882 Å, while the Ni–Cl bond lengths ranged from 2.1829 to 2.2049 Å, consistent with similar compounds.³⁶ On the other hand, the P–Ni bond lengths varied from 2.1533 to 2.1934 Å depending on the substituent of the phosphine group: *di*terbutyl groups resulted in longer bonds and *di*isopropyl or

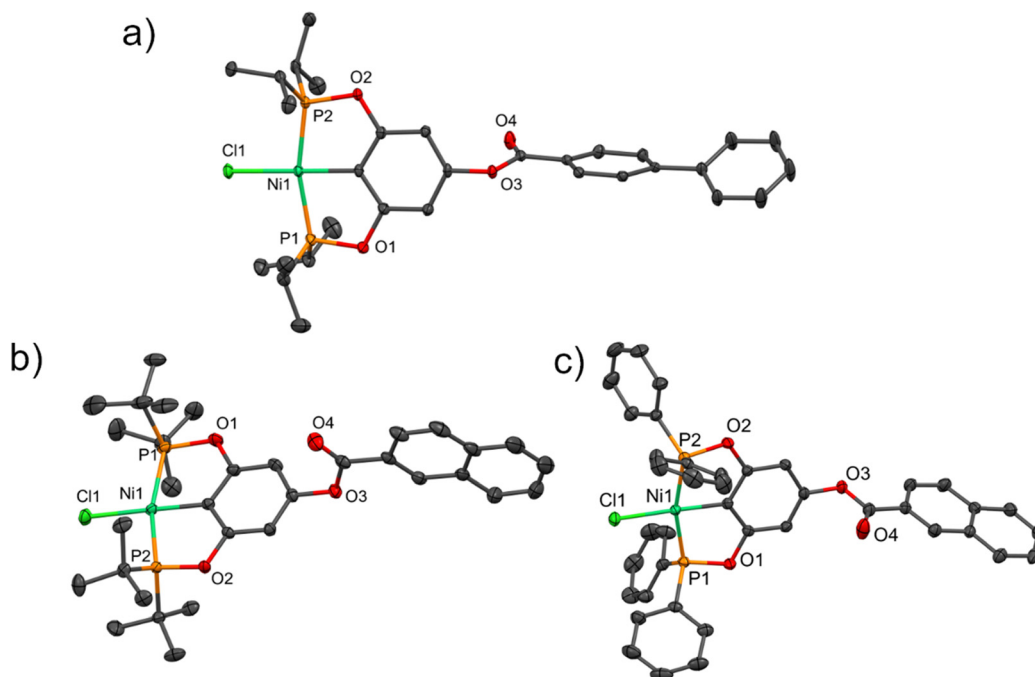


Fig. 1 Molecular structures of compounds (a) 4, (b) 8, and (c) 9. Thermal ellipsoids are drawn at a 30% probability level, the disordered part (compound 8), hydrogen atoms and solvent molecules are omitted for clarity.



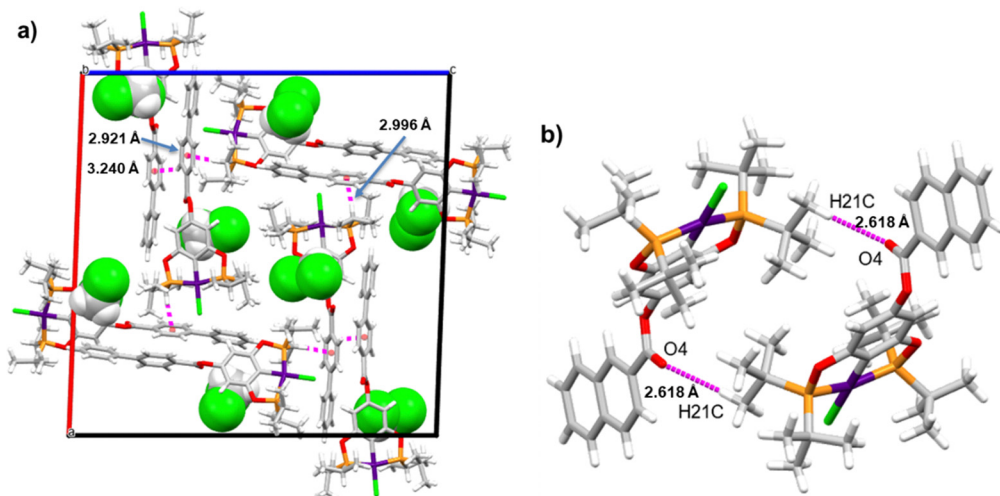


Fig. 2 (a) Crystal packing of **4** and (b) the dimeric structure interaction of compound **8**.

diphenyl produced shorter bonds. The angles between the two atoms in the *trans* positions around nickel (\angle C–Ni–Cl and \angle P–Ni–P) were close to a linear angle of 180° (Table S2, ESI[†]).

Supramolecular analysis of non-covalent interactions

Supramolecular structures are supported *via* CH $\cdots\pi$, O \cdots H, and CH \cdots Cl non-covalent interactions (Table S3, ESI[†]). Three kinds of CH $\cdots\pi$ interactions support the crystal packing of complex **4**, in addition, the molecules of solvent (DCM) are in alternate positions, interacting *via* a CH \cdots O interaction with the oxygen of the ester (Fig. 2a). A dimeric interaction supported by two reciprocal O \cdots H interactions by the ester bridge was observed for the most stable conformation of complex **8** (Fig. 2b). Similarly, two dimeric interactions were observed in complex **9** this time both supported by CH $\cdots\pi$ interactions (Fig. 3a and b). Despite the three complexes containing many aromatic fragments, no π – π stacking was observed.

Hirshfeld surface analysis

For more clarity, we examined the nature of intermolecular interactions of the molecular structure using CrystalExplorer³⁷

software. Hirshfeld surface analysis and two-dimensional fingerprint plots³⁸ for the three compounds (Fig. 5a) were computed. The principal interactions (red regions) on the surface (close contacts) were due to O \cdots H/H \cdots O, and other (H \cdots H, H \cdots C/C \cdots H) interactions are highlighted by conventional mapping of d_{norm} on molecular Hirshfeld surfaces for the three complexes in Fig. 4. For compound **4**, the surface was created for a single molecule of the pincer unity, while for **8** all orientations of the disordered molecule with their partial occupancies were included. Reciprocal O \cdots H/H \cdots O, C \cdots H/H \cdots C, and Cl \cdots H/H \cdots Cl contacts were represented in complex **9** as two symmetrical wings in the fingerprint decomposed plots (Fig. 5b). The most predominant interactions in all the complexes were H \cdots H contacts (see Table 1 and Fig. 6).

Catalytic activity

Among cross-coupling reactions catalyzed by transition metals, C–S couplings have a significant importance to the pharmaceutical industry, enabling the production of a wide variety of important bioactive sulfur compounds such as truxal, metixene and nelfinavir, for instance.^{39–44} Because of this, the study of C–

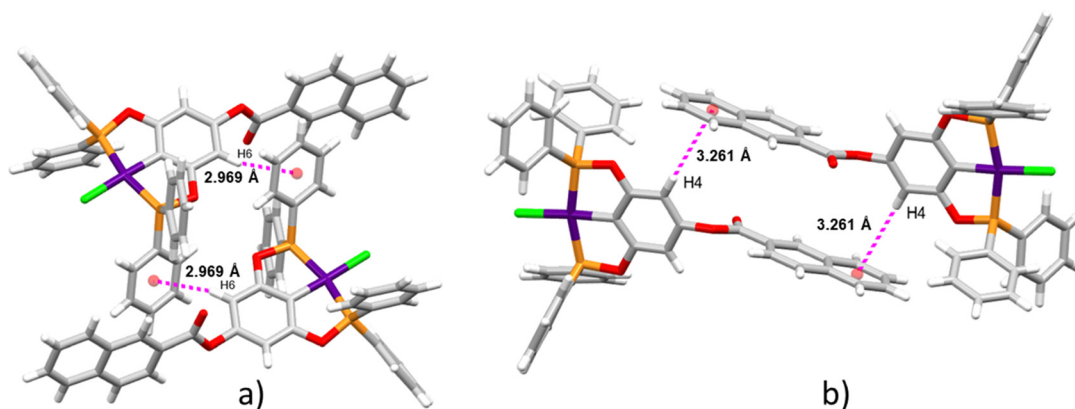


Fig. 3 Two dimeric interactions for complex **9** *via* CH $\cdots\pi$.



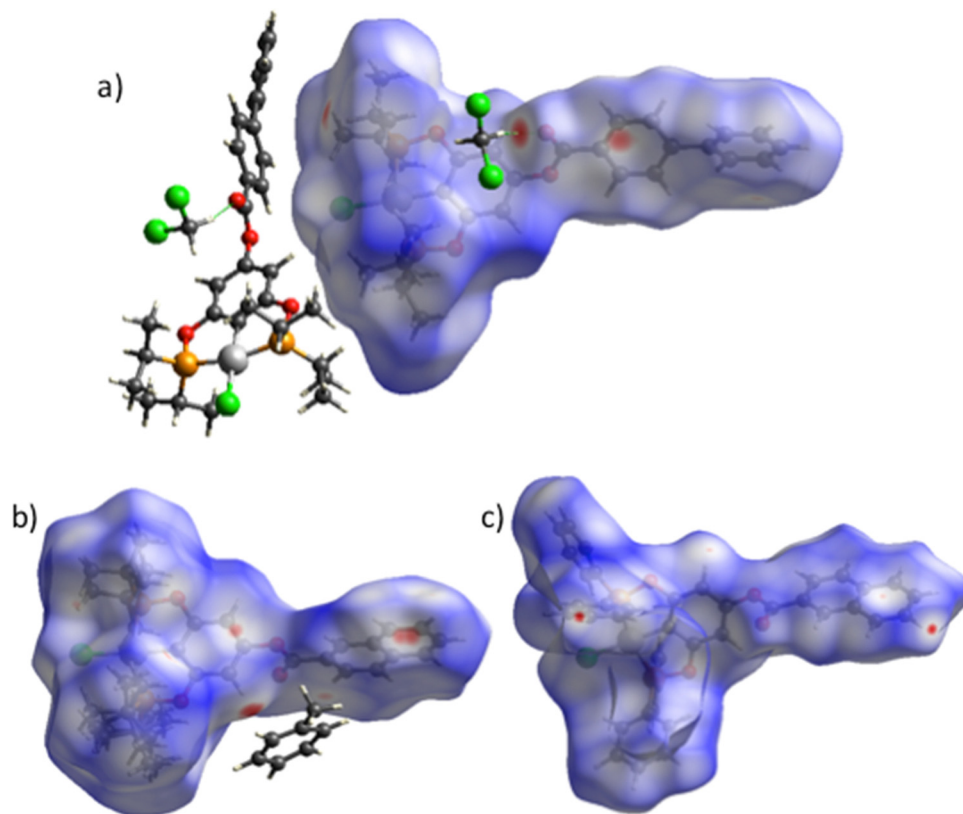


Fig. 4 Hirshfeld surface mapped over d_{norm} for compounds (a) **4** (b) **8** and (c) **9**.

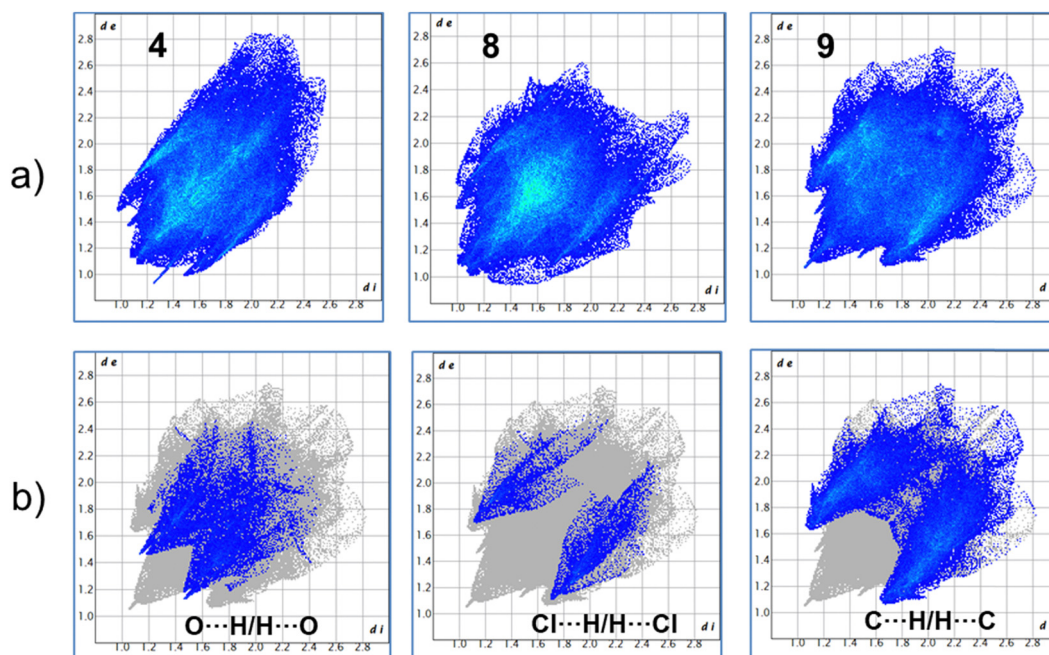


Fig. 5 (a) Fingerprints of complexes **4**, **8** and **9**. (b) Representative decomposed fingerprint plots for compound **9**.

S bonds formation has attracted increasing interest, leading to the development of efficient methodologies for the production of these compounds utilizing transition metal catalysts.

Particularly, catalytic cross-couplings of aryl halides and aryl thiols offer a simple and efficient route for the synthesis of diaryl sulfides and they have been developed using various



Table 1 Principal contacts in compounds **4**, **8** and **9**

	O...H (%)	Cl...H (%)	C...H (%)	H...H (%)	Others (%)
4	8.6	10.7	14.9	62.1	3.7
8	10.2	5.7	33.5	45.0	5.6
9	7.2	3.0	17.8	71.3	0.7

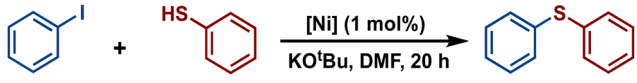
metal-based catalysts such as Co,^{45,46} Cu,^{47,48} Pd,^{49,50} and Ni.^{51,52} Hence, considering that some Ni(II)-POCOP pincer complexes have been successfully employed as catalysts for catalytic C–S coupling reactions^{53–56} we decided to explore the scope of a series of novel *para*-poly-aromatic nickel POCOP-pincer complexes **4–9** in the thiolation of iodobenzene under the optimized reaction conditions previously established in our laboratory using analogous catalytic systems.

The catalytic activity of complexes **1–9** was evaluated in the C–S cross-coupling reaction. All nickel complexes were screened in the coupling reaction of iodobenzene with thiophenol (selected as the model reaction) using KO^tBu as base in DMF at 110 °C for 20 h. Blank tests showed no significant activity without the Ni-POCOP catalyst (<0.5%). The results are summarized in Table 2. In general, all compounds, with the exception of complexes **4** and **2**, demonstrated to be efficient catalysts in this process affording the coupled product (thioether) in high yields (87–100%). Regarding the functionalized complexes, the highest conversions were achieved with complexes **7** and **8**. Interestingly, a comparison between complex **7** (99% yield) and its related non-substituted Ni-POCOP pincer complex **1** (100% yield) under the optimized reactions conditions afforded a very similar catalytic performance. Furthermore, the catalytic activity of complex **2** was significantly increased from 12% yield to 97% (**5**) and 99% (**8**) yield after functionalization with biphenyl and naphthyl fragments.

Encouraged by these results, we turned our attention to extend the scope of this reaction using a series of aromatic and aliphatic thiol derivatives and complex **7** as a catalyst (Table 3).

The variation of the electronic and steric nature of the aryl thiol had an impact on the reaction efficiency and as a result, aromatic thiols with both electron-donating and electron-withdrawing substituents at the *ortho*-position, such as **2b** and **2c** afforded the coupling product in a high yield (Table 3, entries 2 and 3), while those bearing an electron-withdrawing and sterically hindered substituent in the same position provided a low yield (48%, entry 6). On the other hand, simple

Table 2 Cross-coupling reaction of iodobenzene and thiophenol catalysed by nickel complexes **1–9**^a

		
Entry	[Ni]	GC yield ^b (%)
1	1	100
2	2	12
3	3	100
4	4	45
5	5	97
6	6	98
7	7	99
8	8	99
9	9	87

^a Reaction conditions: 0.25 mmol of iodobenzene, 0.25 mmol of thiophenol, 0.25 mmol of KO^tBu, 5 mL of DMF, 1 mol% of catalyst, 110 °C for 20 h. ^b Conversions were obtained by GC-MS and are based on residual iodobenzene and are the average of two runs.

aromatic thiols such as 2-mercapto naphthalene (**2a**) and the *para*-substituted (**2e**) reacted extremely well with iodobenzene, forming the appropriate products in high yields (Table 3, entries 1 and 5). Di-substituted aryl thiols are readily tolerated, and the desired products were obtained in good and excellent yields (entries 7, 8 and 9). In addition, to extend the study of C–S couplings, alkyl thiols were used. They were shown to be less effective than aromatic one, affording the coupling products in low yields (Table 3, entries 10–12). However, it is worth mentioning that the most sterically hindered alkyl thiol offered the best conversion (34%) among these substrates. These results clearly show the efficiency of C–S couplings to be strongly dependent on the sterics of the thiol precursor.

Conclusions

In summary, we report the facile synthesis of six novel *para*-poly-aromatic acyl-functionalized nickel POCOP-pincer complexes, [NiCl{C₆H₂-4-OH-2,6-(OPR₂)₂}] (R = ⁱPr, ^tBu, Ph) in good yields. All the *para*-functionalized nickel pincer complexes are air- and moisture-stable and were fully characterized by NMR spectroscopy, mass spectrometry and elemental analysis. In addition, the molecular structures of complexes **4**, **8** and **9** were unequivocally determined by single crystal X-ray diffraction studies, confirming the tridentate coordination of the pincer ligands. The catalytic activity of all the nickel complexes was

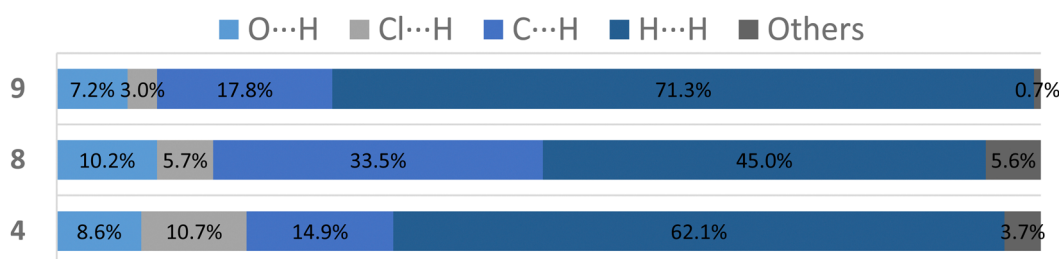
Fig. 6 Plot of percentages of contacts observed in complexes **4**, **8** and **9**.

Table 3 C–S cross-coupling reaction catalyzed by complex 7^a

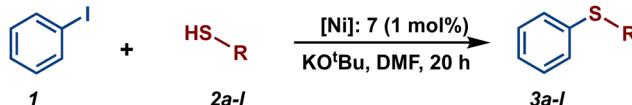
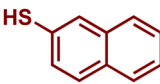
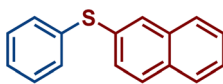
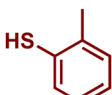
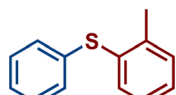
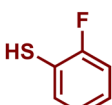
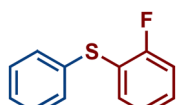
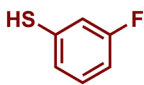
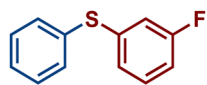
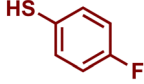
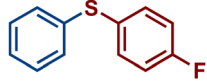
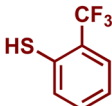
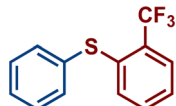
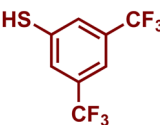
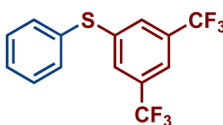
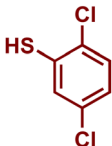
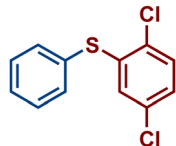
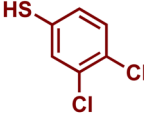
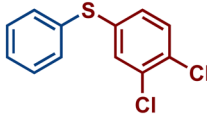
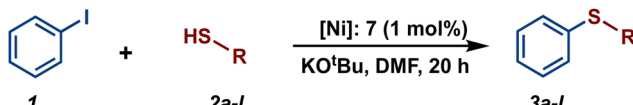

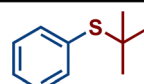
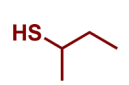
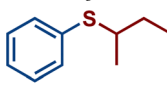
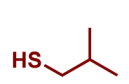
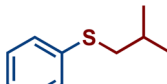
			
Entry	Thiol	Product	GC yield ^b (%)
1			99
	2a	3a	
2			90
	2b	3b	
3			89
	2c	3c	
4			64
	2d	3d	
5			99
	2e	3e	
6			48
	2f	3f	
7			96
	2g	3g	
8			99
	2h	3h	
9			82
	2i	3i	

Table 3 (continued)

			
Entry	Thiol	Product	GC yield ^b (%)
10			34
	2j	3j	
11			5
	2k	2i	
12			7
	2l	2l	

^a Reaction conditions: 0.25 mmol of iodobenzene, 0.25 mmol of thiol, 0.25 mmol of KO^tBu, 2.5 mL of DMF, 1 mol% of catalyst, 110 °C for 20 h. ^b Yields were obtained by GC-MS and are based on residual iodobenzene and are the average of two runs.

evaluated in C–S couplings, exhibiting good performances, except for complex 4. Thus, in general the C–S couplings proceeded well with aryl thiols bearing either electron-withdrawing or electron-donating substituents, while the reactions using alkyl thiols only yielded low conversions. The successful use of these Ni(II) species suggests their potential in other chemical transformations. Thus we are further exploring their catalytic activity in other cross coupling reactions and the potential of the reactivity of the aromatic moieties at the *para* position of the pincer compounds. These results will be disclosed in due course.

Experimental section

All reactions were carried out under nitrogen using standard Schlenk techniques unless otherwise specified. All chemical compounds were obtained from Aldrich Chemical Co. and used as received without further purification. *para*-Hydroxy Ni(II)-POCOP pincer complexes 1, 2 and 3 were synthesized according to the reported procedures and structurally confirmed by direct comparison with literature data. Melting points were recorded on a Mel-Temp II apparatus and are reported without correction. ¹H and ¹³C{¹H} NMR spectra were recorded on a Bruker Ascend 500 spectrometer or on a JEOL GX300 spectrometer. Chemical shifts are reported in ppm down field of TMS using the residual signals in the solvent as the internal standard. Elemental analyses were performed on a PerkinElmer 240 analyzer. MS-Electrospray spectra were recorded on a Bruker Daltonics-Esquire 3000 plus electrospray mass spectrometer. Mass measurements in FAB⁺ were performed at a resolution of



3000 using magnetic field scans and the matrix ions as the reference material or, alternatively, by electric field scans with the sample peak bracketed by two (polyethylene glycol or cesium iodide) reference ions.

General esterification procedure for nickel complexes

A Schlenk flask was charged with the corresponding nickel complex (100 mg) along with NaB(OCH₃)₄ (1.5 eq.) in dry THF (30 mL). The resulting solution was stirred for 2 h at room temperature with an observed color change from yellow to red. Then, the corresponding acyl chloride (1 eq.) was added and the solution returned to its initial color. The reaction mixture was subsequently stirred for 12 h at room temperature. After this time, the solution was evaporated under vacuum and the solid residue was purified by column chromatography using dichloromethane as the eluent. Further removal of the solvent under vacuum yielded the pincer complexes as yellow microcrystalline powders.

Synthesis of 4

Yield: 118 mg (85%). M.p. 262 °C. ¹H NMR (500 MHz, CDCl₃) δ 8.22 (d, ³J_{H-H} = 8.5 Hz, 2H, CH_{Ar}), 7.72 (d, ³J_{H-H} = 8.5 Hz, 2H, CH_{Ar}), 7.65 (d, ³J_{H-H} = 7.1 Hz, 2H, CH_{Ar}), 7.49 (t, ³J_{H-H} = 7.5 Hz, 2H, CH_{Ar}), 7.42 (t, ³J_{H-H} = 7.4 Hz, 1H, CH_{Ar}), 6.37 (s, 2H, CH_{Ar}), 2.43 (q, ³J_{H-H} = 9 Hz, 2H, CH_{Ar}), 2.43 (sept, ³J_{H-H} = 9 Hz, 4H, CH(CH₃)₂), 1.45 (q, ³J_{H-H} = 17.3 Hz, 12H, CH₃), 1.36 (q, ³J_{H-H} = 14.5 Hz, 6H, CH₃). ¹³C{¹H} NMR (126 MHz, CDCl₃) δ 168.4 (t, ²J_{C-P} = 10 Hz, C-OP), 164.9 (s, O=C-O), 151.8 (s, C-O), 146.4 (s, C_{ipso}), 139.7 (s, C_{ipso}), 130.7 (s, CH_{Ar}), 129.1 (s, CH_{Ar}), 128.4 (s, CH_{Ar}), 128.3 (s, CH_{Ar}), 127.4 (s, CH_{Ar}), 127.3 (t, CH_{Ar}), 121.9 (t, ²J_{C-P} = 21 Hz, C-Ni), 99.6 (pt, CH_{Ar}), 27.9 (t, ¹J_{C-P} = 11 Hz, -CH-), 17.6 (s, CH₃), 16.8 (s, CH₃). ³¹P{¹H} NMR (202 MHz, CDCl₃): δ 187.21. MS (DART +): 631 m/z [M]⁺. IR (ATR, cm⁻¹): 2962 (m), 2869 (w), 1728 (s), 1259 (m), 485 (m). Elem. anal. calcd for C₃₁H₃₉ClNiO₄P₂: C, 58.94; H, 6.22. Found: C, 58.92; H, 6.18.

Synthesis of 5

Yield: 120 mg (89%). M.p. 273–274 °C. ¹H NMR (500 MHz, CDCl₃) δ 8.22 (d, ³J_{H-H} = 8.5 Hz, 2H, CH_{Ar}), 7.72 (d, ³J_{H-H} = 8.5 Hz, 2H, CH_{Ar}), 7.66 (d, ³J_{H-H} = 7 Hz, 2H, CH_{Ar}), 7.50–7.47 (m, 2H, CH_{Ar}), 7.43–7.40 (m, 2H, CH_{Ar}), 6.38 (s, 2H, CH_{Ar}), 1.51 (vt, 36H, -CH₃). ¹³C{¹H} NMR (126 MHz, CDCl₃) δ 169.0 (t, ²J_{C-P} = 9 Hz, C-OP), 164.9 (s, O=C-O), 151.5 (s, C-O), 146.4 (s, C_{ipso}), 139.9 (s, C_{ipso}), 130.7 (s, CH_{Ar}), 129.1 (s, CH_{Ar}), 128.4 (s, CH_{Ar}), 127.4 (s, CH_{Ar}), 127.3 (s, CH_{Ar}), 121.4 (t, ²J_{C-P} = 21 Hz, C-Ni), 99.2 (t, ³J_{C-P} = 6 Hz, CH_{Ar}), 39.4 (s, ¹J_{C-P} = 6 Hz, C(CH₃)₃), 28.1 (s, CH₃). ³¹P{¹H} NMR (202 MHz, CDCl₃): δ 189.7. MS (DART +): 688 m/z [M]⁺. IR (ATR, cm⁻¹): 2951 (m), 2855 (w), 1726 (s), 1255 (m), 473 (m). Elem. anal. calcd for C₃₅H₄₇ClNiO₄P₂: C, 61.12; H, 6.89. Found: C, 61.14; H, 6.92.

Synthesis of 6

Yield: 104 mg (80%). M.p. 269–270 °C. ¹H NMR (500 MHz, CDCl₃) δ 8.23 (d, ³J_{H-H} = 8.5 Hz, 2H, CH_{Ar}), 8.03–7.99 (m, 8H, CH_{Ar}), 7.73 (d, ³J_{H-H} = 8.5 Hz, 2H, CH_{Ar}), 7.66 (d, ³J_{H-H} = 7.1 Hz,

2H, CH_{Ar}), 7.55–7.47 (m, 14H, CH_{Ar}), 7.42 (t, ³J_{H-H} = 7.3 Hz, 1H, CH_{Ar}), 6.58 (s, 2H, CH_{Ar}). ¹³C{¹H} NMR (126 MHz, CDCl₃) δ 166.9 (t, ²J_{C-P} = 11.8 Hz, C-OP), 164.9 (s, O=C-O), 152.5 (s, C-O), 146.5 (s, C_{ipso}), 139.9 (s, C_{ipso}), 132.0 (s, CH_{Ar}), 129.1 (s, CH_{Ar}), 128.9 (s, CH_{Ar}), 128.4 (s, CH_{Ar}), 128.1 (s, CH_{Ar}), 127.4 (s, CH_{Ar}), 127.3 (s, CH_{Ar}), 123.2 (t, ²J_{C-P} = 24 Hz, C-Ni), 101.1 (t, ³J_{C-P} = 6.7 Hz, CH_{Ar}). ³¹P{¹H} NMR (202 MHz, CDCl₃): δ 142.8. MS (ESI+): 766 m/z [M]⁺. IR (ATR, cm⁻¹): 2922 (m), 2853 (w), 1735 (s), 1577 (m), 1250 (m), 480 (m). Elem. anal. calcd for C₄₃H₃₁ClNiO₄P₂: C, 67.27; H, 4.07. Found: C, 67.25; H, 4.09.

Synthesis of 7

Yield: 107 mg (85%). M.p. 279–280 °C. ¹H NMR (500 MHz, CDCl₃) δ 8.73 (s, 1H, CH_{Ar}), 8.15 (dd, ³J_{H-H} = 8.6 Hz, ⁴J_{H-H} = 1.7 Hz, 1H, CH_{Ar}), 7.98 (d, ³J_{H-H} = 8.0 Hz, 1H, CH_{Ar}), 7.93 (d, ³J_{H-H} = 8.7 Hz, 1H, CH_{Ar}), 7.91 (d, ³J_{H-H} = 8.2 Hz, 1H, CH_{Ar}), 7.65–7.61 (m, 1H, CH_{Ar}), 7.60–7.55 (m, 1H, CH_{Ar}), 6.60 (m, 2H, CH_{Ar}), 2.44 (sept, ³J_{H-H} = 9 Hz, 4H, CH(CH₃)₂), 1.45 (q, ³J_{H-H} = 17.3 Hz, 12H, CH₃), 1.36 (q, ³J_{H-H} = 14.5 Hz, 12H, CH₃). ¹³C{¹H} NMR (126 MHz, CDCl₃) δ 168.5 (t, ²J_{C-P} = 9 Hz, C-OP), 165.1 (s, O=C-O), 151.8 (s, C-O), 135.9 (s, C_{ipso}), 132.6 (s, CH_{Ar}), 132.0 (s, CH_{Ar}), 129.6 (s, CH_{Ar}), 128.7 (s, CH_{Ar}), 128.5 (s, CH_{Ar}), 127.9 (s, CH_{Ar}), 126.9 (s, CH_{Ar}), 126.8 (s, CH_{Ar}), 125.4 (s, CH_{Ar}), 122.0 (t, ¹J_{C-P} = 21 Hz, CNi), 99.6 (t, ³J_{C-P} = 6 Hz), 27.9 (t, ¹J_{C-P} = 11 Hz, -CH-), 17.6 (s, CH₃), 16.8 (s, CH₃). ³¹P{¹H} NMR (202 MHz, CDCl₃): δ 187.20. MS (DART +): 605 m/z [M]⁺. IR (ATR, cm⁻¹): 2960 (m), 2870 (w), 1722 (s), 1267 (m), 479 (m). Elem. anal. calcd for C₂₉H₃₇ClNiO₄P₂: C, 57.81; H, 6.16. Found: C, 57.83; H, 6.15.

Synthesis of 8

Yield: 108 mg (81%). M.p. 250–251 °C. ¹H NMR (500 MHz, CDCl₃) δ 8.73 (s, 1H, CH_{Ar}), 8.15 (dd, ³J_{H-H} = 8.6 Hz, ⁴J_{H-H} = 1.6 Hz, 1H, CH_{Ar}), 7.98 (d, ³J_{H-H} = 8.1 Hz, 1H, CH_{Ar}), 7.94 (d, ³J_{H-H} = 8.9 Hz, 1H, CH_{Ar}), 7.91 (d, ³J_{H-H} = 8.1 Hz, 1H, CH_{Ar}), 7.65–7.61 (m, 1H, CH_{Ar}), 7.60–7.56 (m, 1H, CH_{Ar}), 6.41 (s, 2H, CH_{Ar}), 1.51 (m, 36H, -CH₃). ¹³C{¹H} NMR (126 MHz, CDCl₃) δ 169.1 (t, ²J_{C-P} = 9 Hz, C-OP), 165.2 (s, O=C-O), 151.5 (s, C-O), 135.9 (s, C_{ipso}), 132.6 (s, CH_{Ar}), 132.0 (s, CH_{Ar}), 129.6 (s, CH_{Ar}), 128.7 (s, CH_{Ar}), 128.5 (s, CH_{Ar}), 127.9 (s, CH_{Ar}), 126.9 (s, CH_{Ar}), 125.5 (s, CH_{Ar}), 121.5 (t, ¹J_{C-P} = 21 Hz, CNi), 99.2 (t, ³J_{C-P} = 6 Hz), 35.5 (t, ¹J_{C-P} = 7 Hz, -C(CH₃)₃), 28.13 (s, CH₃). ³¹P{¹H} NMR (202 MHz, CDCl₃): δ 189.7. MS (DART+): 661 m/z [M]⁺. IR (ATR, cm⁻¹): 2961 (m), 2866 (w), 1735 (s), 1259 (m), 475 (m). Elem. anal. calcd for C₃₃H₄₅ClNiO₄P₂: C, 59.89; H, 6.85. Found: C, 59.95; H, 6.81.

Synthesis of 9

Yield: 110 mg (85%). M.p. 276–277 °C. ¹H NMR (500 MHz, CDCl₃) δ 8.76 (s, 1H, CH_{Ar}), 8.16 (dd, ³J_{H-H} = 8.6 Hz, ⁴J_{H-H} = 1.7 Hz, 1H, CH_{Ar}), 8.05–7.98 (m, 9H, CH_{Ar}), 7.94 (d, ³J_{H-H} = 8.7 Hz, 1H, CH_{Ar}), 7.92 (d, ³J_{H-H} = 8.2 Hz, 1H, CH_{Ar}), 7.66–7.61 (m, 1H, CH_{Ar}), 7.60–7.56 (m, 1H, CH_{Ar}), 7.56–7.46 (m, 12H, CH_{Ar}), 6.41 (s, 2H, CH_{Ar}). ¹³C{¹H} NMR (126 MHz, CDCl₃) δ 166.9 (t, ²J_{C-P} = 12 Hz, C-OP), 165.2 (s, O=C-O), 152.6 (s, C-O), 135.9 (s, C_{ipso}), 132.6 (s, CH_{Ar}), 132.5 (s, CH_{Ar}), 132.3 (s, CH_{Ar}), 132.1 (s, CH_{Ar}), 132.0 (s, CH_{Ar}), 131.9 (s, CH_{Ar}), 129.6 (s, CH_{Ar}),



129.0 (s, CH_{Ar}), 128.9 (s, CH_{Ar}), 128.8 (s, CH_{Ar}), 128.5 (s, CH_{Ar}), 127.9 (s, CH_{Ar}), 127.0 (s, CH_{Ar}), 126.6 (s, CH_{Ar}), 125.5 (s, CH_{Ar}), 123.2 (t, ¹J_{C-P} = 24 Hz, CNi), 101.2 (t, ³J_{C-P} = 7 Hz), ³¹P{¹H} NMR (202 MHz, CDCl₃): δ 142.7. MS (DART +): 741 *m/z* [M]⁺. IR (ATR, cm⁻¹): 2960 (m), 2855 (w), 1734 (s), 1260 (m), 474 (m). Elem. anal. calcd for C₄₁H₂₉ClNiO₄P₂: C, 66.39; H, 3.94. Found: C, 66.37; H, 3.90.

Catalytic experiments

Under nitrogen atmosphere, a solution of KO^tBu (0.25 mmol) and the corresponding nickel catalyst (1 mol%) in DMF (5 mL) was stirred at ambient temperature for 10 min. Then, iodobenzene (0.25 mmol) and the respective thiol (0.25 mmol) were added to the solution. The reaction was heated at 110 °C for the desired time. The reaction mixture was cooled to room temperature and the organic phase analyzed by gas chromatography (GC-MS) (quantitative analyses were performed on an Agilent 6890 N GC with a 30.0 m DB-1MS capillary column coupled to an Agilent 5973 Inert Mass Selective detector).

Data collection and refinement for 4, 8 and 9

Crystals of 4, 8 and 9 were mounted on glass fibers, then placed on a Bruker Smart Apex II diffractometer with a Mo-target X-ray source (λ = 0.71073 Å). The detector was placed at a distance of 5.0 cm from the crystals and frames were collected with a scan width of 0.5 in ω and an exposure time of 10 s frame⁻¹. Frames were integrated with the Bruker SAINT software package using a narrow-frame integration algorithm.⁵⁷ Non-systematic absences and intensity statistics were used in a monoclinic system and P₂₁/n space groups, in all cases. The structures were solved using Patterson methods using the SHELXS-2014/7 program.⁵⁸ The remaining atoms were located *via* a few cycles of least squares refinements and difference Fourier maps. Hydrogen atoms were inputted at calculated positions and allowed to ride on the atoms to which they are attached. Thermal parameters were refined for hydrogen atoms on the phenyl groups using a U_{eq} = 1.2 Å² to the precedent atom. The final cycles of refinement were carried out on all non-zero data using SHELXL-2014/7. Absorption corrections were applied using a SADABS program.⁵⁹ In compound 8, the fragment 'Bu₂P and one molecule of toluene are disordered and were modelled and refined anisotropically in two positions using a variable site occupational factor (SOF), the ratio of SOF was 0.5/0.5.

Data availability

The data supporting this article has been included as part of the ESI.†

Conflicts of interest

There are no conflicts to declare.

Acknowledgements

We would like to thank Chem. Eng. Luis Velasco Ibarra, Dr Francisco Javier Pérez Flores, Q. Eréndira García Ríos, M.Sc. Lucia de Carmen Márquez Alonso, M.Sc. Lucero Ríos Ruiz, M.Sc. Alejandra Núñez Pineda (CCIQS), Q. María de la Paz Orta Pérez, Q. Rocío Patiño-Maya and PhD Nuria Esturau Escofet for technical assistance. E. R. F. would like to thank Programa de Becas Posdoctorales-DGAPA-UNAM for postdoctoral scholarships (Oficio: CJIC/CTIC/4851/2021). The financial support of this research by PAPIIT-DGAPA-UNAM (PAPIIT IN223323) and CONACYT A1-S-033933 is gratefully acknowledged.

References

- 1 D. Morales-Morales, *Rev. Soc. Quím. Mex.*, 2004, **48**, 338–346.
- 2 D. Morales-Morales and C. M. Jensen, *The Chemistry of Pincer Compounds*, Elsevier, 2007.
- 3 D. Morales-Morales, *Mini-Rev. Org. Chem.*, 2008, **5**, 141–152.
- 4 J. Serrano-Becerra and D. Morales-Morales, *Curr. Org. Synth.*, 2009, **6**, 169–192.
- 5 D. F. Brayton, P. R. Beaumont, E. Y. Fukushima, H. T. Sartain, D. Morales-Morales and C. M. Jensen, *Organometallics*, 2014, **33**, 5198–5202.
- 6 M. Asay and D. Morales-Morales, *Dalton Trans.*, 2015, **44**, 17432–17447.
- 7 D. Morales-Morales, *Pincer Compounds Chemistry and Applications*, Elsevier, 2018.
- 8 H. Valdés, M. A. García-Eleno, D. Canseco-Gonzalez and D. Morales-Morales, *ChemCatChem*, 2018, **10**, 3136–3172.
- 9 L. González-Sebastián and D. Morales-Morales, *J. Organomet. Chem.*, 2019, **893**, 39–51.
- 10 H. Valdés, E. Rufino-Felipe and D. Morales-Morales, *J. Organomet. Chem.*, 2019, **898**, 120864.
- 11 A. Mukherjee and D. Milstein, *ACS Catal.*, 2018, **8**, 11435–11469.
- 12 V. Arora, H. Narjinari, P. G. Nandi and A. Kumar, *Dalton Trans.*, 2021, **50**, 3394–3428.
- 13 Z. Wang and N. Liu, *Eur. J. Inorg. Chem.*, 2012, 901–911.
- 14 N. Selander and K. J. Szabó, *Chem. Rev.*, 2011, **111**, 2048–2076.
- 15 A. Kasera, J. P. Biswas, A. Ali Alshehri, S. Ahmed Al-Thabaiti, M. Mokhtar and D. Maiti, *Coord. Chem. Rev.*, 2023, **475**, 214915.
- 16 G. van Koten, *J. Organomet. Chem.*, 2013, **730**, 156–164.
- 17 H. Valdés, L. González-Sebastián and D. Morales-Morales, *J. Organomet. Chem.*, 2017, **845**, 229–257.
- 18 M. A. W. Lawrence, K.-A. Green, P. N. Nelson and S. C. Lorraine, *Polyhedron*, 2018, **143**, 11–27.
- 19 J. W. J. Knapen, A. W. V. D. Made, J. C. D. Wilde, P. W. N. M. V. Leeuwen, P. Wijkens, D. M. Grove and G. V. Koten, *Nature*, 1994, **372**, 659–663.
- 20 G. D. Batema, M. Lutz, A. L. Spek, C. A. V. Walree, C. D. M. Donegá, A. Meijerink, R. W. A. Havenith, J. Pérez-Moreno, K. Clays, M. Büchel, A. V. Dijken, D. L. Bryce,



- G. P. M. V. Klink and G. V. Koten, *Organometallics*, 2008, **27**, 1690–1701.
- 21 W. J. Sommer, K. Yu, J. S. Sears, Y. Ji, X. Zheng, R. J. Davis, C. D. Sherrill, C. W. Jones and M. Weck, *Organometallics*, 2005, **24**, 4351–4361.
- 22 H. P. Dijkstra, M. D. Meijer, J. Patel, R. Kreiter, G. P. M. van Klink, M. Lutz, A. L. Spek, A. J. Canty and G. V. Koten, *Organometallics*, 2001, **20**, 3159–3168.
- 23 M. Albrecht and G. V. Koten, *Adv. Mater.*, 1999, **11**, 171–174.
- 24 J. W. J. Knapen, A. W. van der Made, J. C. de Wilde, P. W. N. M. van Leeuwen, P. Wijkens, D. M. Grove and G. V. Koten, *Nature*, 1994, **372**, 659–663.
- 25 W. T. S. Huck, F. C. J. M. V. Veggel, S. S. Sheiko, M. Möller and D. N. Reinhoudt, *J. Phys. Org. Chem.*, 1998, **11**, 540–545.
- 26 M. Albrecht and G. v Koten, *Adv. Mater.*, 1999, **11**, 171–174.
- 27 M. Albrecht, R. A. Gossage, M. Lutz, A. L. Spek and G. V. Koten, *Chem. – Eur. J.*, 2000, **6**, 1431–1445.
- 28 H.-J. V. Manen, R. H. Fokkens, N. M. M. Nibbering, F. C. J. M. V. Veggel and D. N. Reinhoudt, *J. Org. Chem.*, 2001, **66**, 4643–4650.
- 29 G. Rodríguez, M. Albrecht, J. Schoenmaker, A. Ford, M. Lutz, A. L. Spek and G. V. Koten, *J. Am. Chem. Soc.*, 2002, **124**, 5127–5138.
- 30 K. Yu, W. Sommer, M. Weck and C. Jones, *J. Catal.*, 2004, **226**, 101–110.
- 31 H. P. Dijkstra, M. D. Meijer, J. Patel, R. Kreiter, G. P. M. V. Klink, M. Lutz, A. L. Spek, A. J. Canty and G. V. Koten, *Organometallics*, 2001, **20**, 3159–3168.
- 32 D. E. Bergbreiter, Philip L. Osburn and Y.-S. Liu, *J. Am. Chem. Soc.*, 1999, **121**, 9531–9538.
- 33 M. Q. Slagt, D. A. P. v Zwielen, A. J. C. M. Moerkerk, R. J. M. K. Gebbink and G. V. Koten, *Coord. Chem. Rev.*, 2004, **248**, 2275–2282.
- 34 M. A. García-Eleno, E. Padilla-Mata, F. Estudiante-Negrete, F. Pichal-Cerda, S. Hernández-Ortega, R. A. Toscano and D. Morales-Morales, *New J. Chem.*, 2015, **39**, 3361–3365.
- 35 M. A. García-Eleno, M. Quezada-Miriel, R. Reyes-Martínez, S. Hernández-Ortega and D. Morales-Morales, *Acta Crystallogr., Sect. C: Cryst. Struct. Commun.*, 2016, **72**, 393–397.
- 36 A. A. Castillo-García, L. González-Sebastián, L. Lomas-Romero, S. Hernández-Ortega, R. A. Toscano and D. Morales-Morales, *New J. Chem.*, 2021, **45**, 10204–10216.
- 37 P. R. Spackman, M. J. Turner, J. J. McKinnon, S. K. Wolff, D. J. Grimwood, D. Jayatilaka and M. A. Spackman, *J. Appl. Cryst.*, 2021, **54**, 1006–1011.
- 38 A. Parkin, G. Barr, W. Dong, C. J. Gilmore, D. Jayatilaka, J. J. McKinnon, M. A. Spackman and C. C. Wilson, *CrystrEngComm*, 2007, **9**, 648–652.
- 39 K. A. Scott and J. T. Njardarson, *Top. Curr. Chem.*, 2018, **376**, 5.
- 40 G. D. Martino, M. C. Edler, G. L. Regina, A. Coluccia, M. C. Barbera, D. Barrow, R. I. Nicholson, G. Chiosis, A. Brancale, E. Hamel, M. Artico and R. Silvestri, *J. Med. Chem.*, 2006, **49**, 947–954.
- 41 G. Evano, C. Theunissen and A. Pradal, *Nat. Prod. Rep.*, 2013, **30**, 1467–1489.
- 42 E. A. Ilardi, E. Vitaku and J. T. Njardarson, *J. Med. Chem.*, 2014, **57**, 2832–2842.
- 43 C. F. Lee, Y. C. Liu and S. S. Badsara, *Chem. – Asian J.*, 2014, **9**, 706–722.
- 44 D. A. Boyd, *Angew. Chem., Int. Ed.*, 2016, **55**, 15486–15502.
- 45 Y.-C. Wong, T. T. Jayanth and C.-H. Cheng, *Org. Lett.*, 2006, **8**, 5613–5616.
- 46 M.-T. Lan, W.-Y. Wu, S.-H. Huang, K.-L. Luo and F.-Y. Tsai, *RSC Adv.*, 2011, **1**, 1751–1755.
- 47 D. Andrada, S. Soria-Castro, D. Caminos, J. Argüello and A. Peñeñory, *Catalysts*, 2017, **7**, 388.
- 48 W.-K. Huang, W.-T. Chen, I. J. Hsu, C.-C. Han and S.-G. Shyu, *RSC Adv.*, 2017, **7**, 4912–4920.
- 49 T. Itoh and T. Mase, *Org. Lett.*, 2004, **6**, 4587–4590.
- 50 M. A. Fernández-Rodríguez, Q. Shen and J. F. Hartwig, *J. Am. Chem. Soc.*, 2006, **128**, 2180–2181.
- 51 Y. Zhang, K. C. Ngeow and J. Y. Ying, *Org. Lett.*, 2007, **9**, 3495–3498.
- 52 X.-B. Xu, J. Liu, J.-J. Zhang, Y.-W. Wang and Y. Peng, *Org. Lett.*, 2013, **15**, 550–553.
- 53 V. Gómez-Benítez, O. Baldovino-Pantaleón, C. Herrera-Álvarez, R. A. Toscano and D. Morales-Morales, *Tetrahedron Lett.*, 2006, **47**, 5059–5062.
- 54 J. Zhang, C. M. Medley, J. A. Krause and H. Guan, *Organometallics*, 2010, **29**, 6393–6401.
- 55 G. T. Venkanna, H. D. Arman and Z. J. Tonzetich, *ACS Catal.*, 2014, **4**, 2941–2950.
- 56 J. M. Serrano-Becerra, H. Valdés, D. Canseco-González, V. Gómez-Benítez, S. Hernández-Ortega and D. Morales-Morales, *Tetrahedron Lett.*, 2018, **59**, 3377–3380.
- 57 Bruker Programs: APEX3, SAINT, Bruker AXS Inc., Madison, Wisconsin, USA, 2018.
- 58 G. M. Sheldrick, Crystal structure refinement with SHELXL, *Acta Crystallogr., Sect. C: Struct. Chem.*, 2015, **71**, 3–8.
- 59 L. Krause, R. Herbst-Irmer, G. M. Sheldrick and D. Stalke, *SADABS 2016/2, J. Appl. Cryst.*, 2015, **48**, 3–10.

